

# Mechanical Strain, Induced Noninvasively in the High-frequency Domain, Is Anabolic to Cancellous Bone, But Not Cortical Bone

C. RUBIN,<sup>1</sup> A. S. TURNER,<sup>2</sup> C. MALLINCKRODT,<sup>2</sup> C. JEROME,<sup>3</sup> K. MCLEOD,<sup>1</sup> and S. BAIN<sup>2</sup>

<sup>1</sup>Musculo-Skeletal Research Laboratory, Department of Biomedical Engineering, State University of New York, Stony Brook, NY, USA

<sup>2</sup>Department of Clinical Sciences, Colorado State University, Fort Collins, CO, USA

<sup>3</sup>Skeletech, Inc., Bothell, WA, USA

Departing from the premise that it is the large-amplitude signals inherent to intense functional activity that define bone morphology, we propose that it is the far lower magnitude, high-frequency mechanical signals that continually barrage the skeleton during longer term activities such as standing, which regulate skeletal architecture. To examine this hypothesis, we proposed that brief exposure to slight elevations in these endogenous mechanical signals would suffice to increase bone mass in those bones subject to the stimulus. This was tested by exposing the hind limbs of adult female sheep ( $n = 9$ ) to 20 min/day of low-level (0.3g), high-frequency (30 Hz) mechanical signals, sufficient to induce a peak of approximately 5 microstrain ( $\mu\epsilon$ ) in the tibia. Following euthanasia, peripheral quantitative computed tomography (pQCT) was used to segregate the cortical shell from the trabecular envelope of the proximal femur, revealing a 34.2% increase in bone density in the experimental animals as compared with controls ( $p = 0.01$ ). Histomorphometric examination of the femur supported these density measurements, with bone volume per total volume increasing by 32% ( $p = 0.04$ ). This density increase was achieved by two separate strategies: trabecular spacing decreased by 36.1% ( $p = 0.02$ ), whereas trabecular number increased by 45.6% ( $p = 0.01$ ), indicating the formation of cancellous bone de novo. There were no significant differences in the radii of animals subject to the stimulus, indicating that the adaptive response was local rather than systemic. The anabolic potential of the signal was evident only in trabecular bone, and there were no differences, as measured by any assay, in the cortical bone. These data suggest that subtle mechanical signals generated during predominant activities such as posture may be potent determinants of skeletal morphology. Given that these strain levels are three orders of magnitude below strains that can damage bone tissue, we believe that a noninvasive stimulus based on this sensitivity has potential for treating skeletal complications such as osteoporosis. (Bone 30:445–452; 2002) © 2002 by Elsevier Science Inc. All rights reserved.

Address for correspondence and reprints: Clinton Rubin, Ph.D., Department of Biomedical Engineering, Psychology-A, Third Floor, State University of New York at Stony Brook, Stony Brook, NY 11794-2580. E-mail: clinton.rubin@sunysb.edu

Preliminary data from this study were published previously as a brief communication (*Nature* 412:603–604; 2001).

**Key Words:** Anabolic; Osteogenic; Mechanical; Trabecular; Osteoporosis; Bone adaptation; Osteoblasts.

## Introduction

A large component of the skeleton's structural success can be attributed to the ability of bone tissue to rapidly accommodate changes in its mechanical environment, thus ensuring that sufficient skeletal mass is appropriately placed to withstand the rigors of functional activity.<sup>52</sup> Consistent with the adaptive potential of bone, extensive, long-term exercise has been shown to increase skeletal mass,<sup>47</sup> and the anabolic potential is realized, to a limited extent, even in the elderly.<sup>22</sup> Although there is consensus that mechanical factors are critical to achieving and retaining the structural reliability of the skeleton, great controversy arises with attempts to identify those specific mechanical parameters responsible for governing bone growth and remodeling.<sup>19</sup>

It is generally believed that the mechanical signals responsible for regulating bone adaptation are those associated with the most vigorous activities.<sup>18</sup> In the extreme case, it has been proposed that bone adaptation itself is mediated not by a "physiologic" response, but rather through the repair of material microdamage accumulated by these extreme deformations.<sup>9</sup> Short of repair, it is as likely that a strain of 2000–3000  $\mu\epsilon$ , typical to the appendicular skeleton during vigorous locomotion,<sup>8,33,36</sup> mediates bone mass and morphology through the highly orchestrated regulation of osteoclast and osteoblast activity to first remove, and then replace, targeted tissue.<sup>46</sup> From either of these perspectives, the intricacies of vertebrate morphology would be closely linked to the intensity of function, with the most extreme activity having the greatest influence on bone girth, curvature, and architecture.<sup>13</sup>

Departing somewhat from a hypothesis that emphasizes a dependence of bone adaptation on peak skeletal strains, we propose that the extremely small strains that arise during less vigorous—but more predominant—activities such as posture<sup>23</sup> may have a potent influence on bone architecture.<sup>40,44</sup> If the skeleton is sensitive to these low, but omnipresent strains, then vertebrate morphology would reflect more subtle, but certainly more common, responsibilities such as standing (axial and appendicular architecture) and talking (cranial architecture<sup>24</sup>). Thus, small decreases in this barrage of regulatory signal would be permissive to resorptive activities (e.g., bedrest, microgravity), whereas small increases in their magnitude, such as those examined herein, would stimulate anabolic activity.

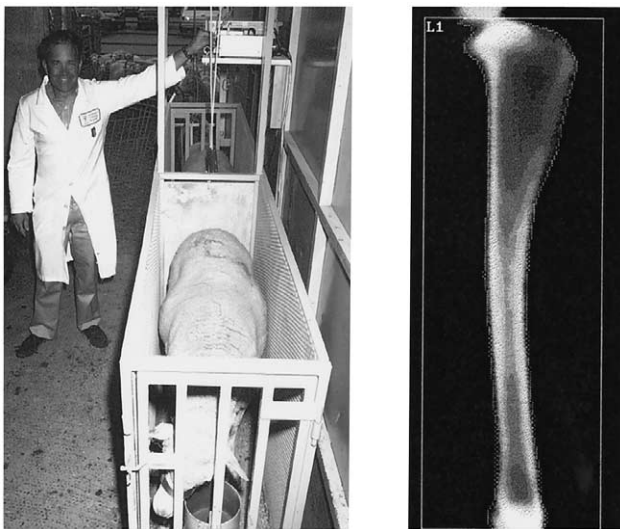


**Figure 1.** Once each day, sheep were brought into one of two constrained chutes for their 20 min mechanical regimen (left). The oscillating device was affixed to the loading frame such that the top surface was flush to the floor of the chute, and only the hind limbs of the animals were subject to the mechanical stimulus. Beginning at baseline, and again at 3, 6, and 12 months, each animal was anesthetized and DXA scans made of the regions of interest (ROIs) of the ultradistal radius and whole tibia (right). To minimize variation, one investigator (A.T.S.) positioned each animal for the scans, and made each measurement, including the determination of the ROI. Scans were made without knowledge of whether the animal was from the experimental or control group.

## Methods

Eighteen adult female sheep (Warhill, intact ewes, 60–80 kg), 6–8 years of age, were randomized into two groups: (1) experimental; and (2) untreated controls. For 20 min/day, 5 days/week, the experimental sheep stood constrained in a chute such that only the hind limbs were subject to a vertical ground-based vibration, oscillating at 30 Hz, to create peak-to-peak accelerations of  $0.3g$  ( $2.9 \text{ m sec}^{-2}$ ;  $1g = \text{earth's gravitational field} = 9.8 \text{ m sec}^{-2}$ ). When the animals were not being treated, they joined the controls to roam freely in a pasture area.

### Noninvasive Mechanical Signal

Oscillation of the experimental animals was achieved using an apparatus that relies on establishing whole body resonance. This noninvasive approach permits the use of small, low force (18 N) actuators (Model LA18-18, BEI, San Marcos, CA) to impose accelerations of up to  $0.6g$  on animals of up to 80 kg over the frequency range of 5–150 Hz.<sup>15</sup> With appropriate accelerometer feedback from the plate surface, control circuitry was capable of eliminating nontranslational modes of vibration due to motion or postural changes of the animal. The forelimbs of the sheep rested on a skirt around the active plate (**Figure 1**, left), allowing the radius to be used as an intra-animal control for dual-energy X-ray absorptiometry (DXA) and histomorphometry measurements.

### Bone Strain Measurements

At the beginning of the protocol, the oscillating device was calibrated by measuring strains from tibiae of two calibration animals. Under general halothane anesthesia using aseptic conditions, three three-element stacked rosette strain gauges (2 mm

gauge length, 120  $\Omega$ ; Model FRA-2-11, TML Gauges, Kenkyujo, Japan) were attached to the left tibial midshaft, a site selected because of the ease in which the three surfaces of the tibia can be exposed with only very minimal musculoskeletal disruption.<sup>16</sup> Exposure of the tibial surface was prepared by removing a small ( $50 \text{ mm}^2$ ) area of the periosteum, drying the exposed surface with anhydrous diethylether, and gluing the gauge to the surface with isobutyl 2-cyanoacrylate monomer (Ethicon, Ltd.). The animals were awake and fully ambulatory within 3 h, and were immediately capable of unrestricted activity.

Each 120  $\Omega$  gauge was conditioned with a 3 V bridge excitation voltage and amplified with a Model 2100 system (Vishay Measurements Group). A bridge amplifier gain of  $1300\times$  was utilized. The amplified analog strain signals were filtered through low-pass antialiasing filters (AAF-8, Keithley Metrabyte) with a cut-off frequency of 50 Hz, and digitized with 16 bit resolution (AT-MIO-16X, National Instruments) at a sampling rate of 102.4 Hz. In this configuration, resolution of the system was better than  $0.1 \mu\epsilon$ , yet strains in the range of  $\pm 2500 \mu\epsilon$  could also be recorded. The filters and A/D board occupied three I/O slots of a 486-DX2 (66 MHz) PC. Data were stored in binary files on the PC's hard disk that included 37 kilobytes each for nine channels of strain signal. The strain caused by the oscillation was digitized in real time and transferred to a RISC-6000 (IBM) workstation storage for analysis.

### Bone Mineral Density

At baseline, 7, 15, 29, 43, and 54 weeks of stimulation, DXA measurements (Model QDR-1000/W, Hologic, Inc., Bedford, MA) were performed on the tibia and ultradistal radius of experimental and control animals to establish bone mineral density (BMD) at these sites (**Figure 1**, right). Due to anatomic constraints, DXA of the femur was not possible. To minimize movement during each scan, animals were subject to general anesthesia. A mixture of 5 mg/kg ketamine (Ketaset, Fort Dodge Laboratories, Inc., Fort Dodge, IA) and 7.5 mg total diazepam (Elkins-Sinn, Inc., Cherry Hill, NJ) was administered intravenously through a catheter in an ear vein and maintained with halothane-oxygen. Scan speed was run at 60 mm/sec, with a line increment of 1 mm. Computer software for determining BMC and BMD was supplied by Hologic (same as used for humans, version 6.10.01).

To minimize variation in positioning and determining regions of interest (ROIs), all DXA measurements were made by one investigator (A.S.T.), and ROIs determined at the time of the scan.<sup>48</sup> In the radius, the ROI of the ultradistal radius was defined as a rectangle extending from the physal scar proximally, whereas BMD and BMC of the tibia were determined using a rectangle that encompassed the entire length of the bone (**Figure 1b**). Short-term precision and machine stability was evaluated prior to each scan series using the anthropomorphic lumbar spine phantom (Hologic), with BMC area and BMD measured prior to scanning of the animals. Precision was defined as coefficient of variation (CV) and expressed as a percentage, where  $CV\% = SD/\text{mean} \times 100$ .

Following the 1 year measurements, the animals were killed and the femora, tibiae, and radii removed, and DXA performed, *ex vivo*, on the left femur of each animal. Peripheral quantitative computed tomography (pQCT; Stratec XCT-3000, Research, Norland Medical Systems, Inc., Fort Atkinson, WI) was then performed on the proximal quarter of the left femur, and this anatomic region was prepared for static and dynamic histomorphometry (the distal femora were prepared for microcomputed tomography and mechanical testing, the results of which have been reported elsewhere<sup>43</sup>). All *in vivo* and *ex vivo* DXA and

pQCT evaluations were performed without knowledge of whether the animals were control or experimental.

### Histomorphometry

Dynamic indices of bone formation from the proximal femur were based on paired labels of the same color administered according to the following “2 days on/12 days off/2 days on” fluorochrome labeling schedule: xylenol orange (15 mg/kg intravenously [IV]) on days 20, 21 and 33, 34; tetracycline (15 mg/kg intramuscularly [IM]) on days 170, 171 and 183, 184; and calcein (15 mg/kg IV) on days 340, 341 and 353, 354.

Following pQCT measurements, the proximal femur and ultradistal radius was fixed for 24 h in cold (4°C) 70% ethanol (EtOH). To prevent decalcification, the bones were dehydrated in an ascending series of EtOH concentrations, ending with three 24 h changes of a solution composed of 85% methylmethacrylate, 10% glycolmethacrylate, 5% dibutylthallate, and 5 g polyethylene glycol disterate with 0.8 g benzoylperoxide per 100 mL. To expedite dehydration and infiltration, samples were gently agitated on a shaker. To embed the bone specimens, JB-4 Solution B (Polysciences) was added to fresh infiltration solution (1 mL/100 mL), and polymerized under a nitrogen atmosphere.<sup>3</sup>

Full transverse sections of the proximal femur and ultradistal radius were cut from the polymerized blocks using a Reichert/Jung Model-K sledge microtome equipped with an HK-2 profile tungsten-carbide knife. Sections for fluorescence microscopy were cut 5 µm thick and mounted unstained on glass slides with Eukitt's media. Sections for light microscopy were cut 5 µm thick, and stained with a modified toluidine blue, which permitted osteoid cement line differentiation from mineralized bone.<sup>2</sup>

The morphometric evaluations of undecalcified sections were performed on a Nikon Labophot equipped for bright-field and epifluorescence microscopy, and reflected light microscopy. To evaluate modeling and/or remodeling events, observations from stained and unstained sections were recorded through the microscope's ocular field via a camera lucida, using a cursor LED interfaced with a digitizing pad and an IBM Pentium-II PC using the OSTEOMEASURE morphometry software program (Osteometrics Corp.). Static parameters evaluated included bone volume relative to total tissue volume, mean trabecular thickness, and trabecular number per unit volume. Dynamic indices evaluated were bone formation rate and mineralizing surface.<sup>31</sup>

### Statistics

In the case of the longitudinal DXA data, mean change in BMD was analyzed with a likelihood-based repeated-measures approach.<sup>26</sup> Fixed effects included in these analyses were treatment, time, treatment × time interaction, and baseline BMD value. Separate analyses were conducted by location (radius vs. tibia). The within-subject errors were modeled using an unstructured covariance matrix. In these analyses, time was considered as a categorical effect, thereby assuming no structural form to trends in BMD over time. The comparisons of primary interest from this analysis were the pairwise contrasts between treatments at each timepoint.

A second analysis was conducted in which time was considered as a continuous effect and BMDs from both locations were included in one analysis. By including the treatment × time × location three-way interaction, the linear trends over time could be compared for each treatment at each location. The unstructured time trend analysis was more general, not assuming any functional form for trends over time. Assuming a linear time trend generally yields a more powerful analysis because comparisons in rate of change are made by incorporating data from

all measurement timepoints, whereas the pairwise contrasts from the analysis in which time was considered categorical are made on a timepoint-by-timepoint basis. However, results from the linear time trend analysis are valid only if a linear time trend describes responses accurately. Percentage change in BMD is a commonly reported response measure. Therefore, analyses of percent change were also conducted. However, *p* values from only the actual change in BMD were reported.

### Results

The anabolic potential of extremely small (0.3g), high-frequency (30 Hz) mechanical signals were examined by subjecting the hind limbs of adult (6–8 years) sheep to 20 min/day, 5 days/week, of ground-based vertical accelerations. Strain gauges attached to the diaphyseal midshaft of the tibia of animals used to calibrate the device showed that this signal generated peak-to-peak strains of no more than 5 µε, one-thousandth of the strain magnitude necessary to cause yield failure in bone.<sup>11</sup>

In the linear time trend analysis of BMD, the difference between treatments in rate of change varied significantly by location (*p* value for three-way interaction of treatment × time × location = 0.038). Consistent with our hypotheses, BMD in tibiae of sheep in the active group increased appreciably, whereas BMD decreased or increased minimally in tibiae of placebo sheep and in the radius of sheep in both experimental and control animals. Least-square means for change in tibial BMD from the unstructured time trend analysis are summarized in **Table 1** by treatment and time. The difference between treatments was significant at 29 weeks and approached significance at week 54. At all timepoints, the active treatment group had a greater mean change in BMD compared with the placebo group. Least-square means for change in radius BMD from the unstructured time trend analysis are summarized in **Table 2** by treatment and time. The differences between treatments did not approach significance at any timepoint.

Using DXA whole bone measurements on excised femora, BMD in the experimental animals was 5.4% greater than in controls (*p* = 0.1; **Table 3**). Tomographic measurements confirmed this trend toward a difference in the femora, as the density of the proximal region of the experimental femora was 6.5% greater than controls (*p* = 0.1).

Algorithms were then used to separate the pQCT measurement to consider only cortical or trabecular bone of the proximal quarter of the femur. When only the cortical shell of the proximal femur was considered, there was no significant difference between control and experimental bones (density levels of the experimental animals were 1.6% less than controls, which was not statistically significant). In contrast, when the endosteal envelope was considered, the density of the trabecular bone in the proximal femur was 34.2% greater in experimental sheep as compared with controls (*p* = 0.01).

The significant differences between control and experimental femora measured using pQCT was substantiated by undecalcified bone histology of the femur (**Table 4**), which demonstrated a 32% increase in trabecular bone volume per total volume (*p* = 0.04), a 45% increase in trabecular number (*p* = 0.01), and a 36% decrease in trabecular spacing (*p* = 0.02; **Figure 2**). There was a slight drop (8%) in the mean thickness of trabeculae (*p* = 0.22). The low-level mechanical stimulation increased bone formation rate 2.1-fold (*p* = 0.19), and mineralizing surface 2.4-fold (*p* = 0.09; **Figure 3**), supporting the significant increases in BMD measured, as a function of time, in the tibia of experimental animals. The anabolic effect was highly selective for cancellous bone as there were no significant histomorphometric changes in any cortical bone parameters (data not shown).

**Table 1.** Dual energy X-ray absorptiometry data for the tibia as a function of time and treatment

Treatment	Mean change	% change	SE	Within	<i>p</i> diff.
Week 7					
Active	−0.019	−0.018	0.026	0.332	0.522
Placebo	−0.036	−0.033	0.018	0.072	
Week 15					
Active	−0.001	−0.001	0.026	0.952	0.345
Placebo	−0.027	−0.024	0.018	0.186	
Week 29					
Active	0.017	0.017	0.022	0.291	0.050
Placebo	−0.030	−0.027	0.015	0.082	
Week 43					
Active	0.041	0.041	0.028	0.061	0.219
Placebo	0.005	0.008	0.019	0.685	
Week 54					
Active	0.043	0.042	0.024	0.026	0.120
Placebo	0.003	0.005	0.017	0.770	

Mean change from baseline repeated measures analysis-timewise LS-means. Significant differences between placebo and active device were observed at 6 months.

Neither static nor dynamic histomorphometry of the ultradistal radius revealed any differences between the control and experimental animals, whether cortical or trabecular bone (Table 4).

## Discussion

Mechanical strain in the skeleton is a product of functional load bearing; strain is evident from the mandible of the macaque<sup>24</sup> to the tibia of the alligator.<sup>6</sup> In addition to the large-amplitude strains typically associated with functional activity,<sup>5</sup> a strain signal, far less than 5  $\mu\epsilon$  in amplitude, arises through muscular activity in the frequency band of 10–50 Hz.<sup>15</sup> These small-amplitude, high-frequency signals persist essentially at all times during which muscle contraction is involved, including passive actions such as standing. Considering the omnipresence of these muscle-induced signals, and considering that high-frequency mechanical strains<sup>40,44</sup> or electric fields<sup>29</sup> can be anabolic to bone even at extremely low magnitudes, we hypothesized that these mechanical signals may represent a key regulatory signal to define the structure of the skeleton.

Proposing that small, persistent strains are influential in the determination of bone architecture does not dismiss large signals

as being unimportant, and certainly large-magnitude (>1000  $\mu\epsilon$ ) low-frequency (1 Hz) mechanical signals have strong osteogenic potential.<sup>37</sup> It is important to emphasize, however, that even though very few large-strain magnitude signals are necessary to influence bone architecture,<sup>38</sup> such large-amplitude signals happen only rarely,<sup>1</sup> even under severe conditions of military training.<sup>10</sup> Therefore, the barrage of signals that arise from more typical activities such as walking or talking would serve as a more dependable source of mechanical information to help define both bone mass and morphology. Moreover, 20 min/day of a 5  $\mu\epsilon$  stimulus at 30 Hz induces 36,000 cycles/day of a stimulus that is, in reality, 20-fold greater than the 30 Hz signal that arises during quiet standing, and thus represents an order of magnitude increase in the total strain energy induced at that frequency over a 12 h period.<sup>15</sup> Thus, even though the applied signal is low relative to peak strain events, when compared with the signals normally experienced at this frequency, they are quite large. Whether this increase at 30 Hz stimulates adaptation because of some preferential sensitivity of bone cells to higher frequency strains,<sup>40</sup> because the sensitivity of the tissue is enhanced by exceeding a threshold of stochastic noise,<sup>23</sup> because this “increase” disrupts the 1/f power law relationship of bone

**Table 2.** Dual energy X-ray absorptiometry data for the ultradistal region of the radius as a function of time and treatment.

Treatment	Mean change	% change	SE	Within	<i>p</i> diff.
Week 7					
Active	−0.010	−0.012	0.015	0.355	0.083
Placebo	−0.038	−0.042	0.010	0.002	
Week 15					
Active	−0.030	−0.035	0.021	0.063	0.297
Placebo	−0.053	−0.061	0.015	0.002	
Week 29					
Active	0.005	0.006	0.015	0.638	0.107
Placebo	−0.032	−0.036	0.010	0.008	
Week 43					
Active	0.001	0.000	0.023	0.996	0.413
Placebo	−0.018	−0.022	0.016	0.213	
Week 54					
Active	−0.017	−0.021	0.022	0.270	0.445
Placebo	−0.035	−0.040	0.015	0.037	

Mean change from baseline repeated measures analysis-timewise LS-means. There were no significant differences from zero, or between treatments.

**Table 3.** Animal mass, bone mineral density (determined by DXA), and envelope-specific density (determined by pQCT) of the proximal femur following 12 months of low-level mechanical stimulation

	Control	Experimental	Difference	P value
<b>DXA</b>				
Animal mass (kg)	71.1 ± 7.1	70.3 ± 9.4	-1.1%	n.s.
Bone mineral density (g/cm <sup>2</sup> )	0.83 ± .06	0.88 ± .05	+5.4%	0.1
<b>pQCT</b>				
Total density (g/cm <sup>3</sup> )	466 ± 60	496 ± 53	+6.5%	0.1
Cortical density (g/cm <sup>3</sup> )	1215 ± 51	1193 ± 49	-1.6%	n.s.
Trabecular density (g/cm <sup>3</sup> )	169 ± 37	227 ± 56	+34.2%	0.01

These data, indicating the anabolic nature of the stimulus, are supported by indices of static and dynamic histomorphometry of the proximal femur (see Table 4). Whereas “whole bone” evaluations of the proximal femur show only a trend of influence by mechanical stimuli ( $p = 0.1$ ), when trabecular bone is considered alone, the “benefit” compared with control is >30% ( $p = 0.01$ ). One control was lost over the course of study for reasons not associated with the protocol. As shown, nine animals were evaluated in the experimental group, and eight in the control group.  
KEY: DXA, dual-energy X-ray absorptiometry; n.s., not significant; pQCT, peripheral quantitative computed tomography.

strain history<sup>15</sup> with the shift itself causing the “self-organized system” of bone to adapt, or — of course — through some other as yet unidentified mechanism, is not clear.

Strain gauges attached to the midshaft of the tibia demonstrated that the 30 Hz, 0.3g oscillation stimulated peak strains of approximately 5  $\mu\epsilon$  on the cortex, several orders of magnitude below those strain levels generated during running or even walking. Even though strains may be accurately quantified from the cortical surface, it is reasonable to assume that the trabeculae within the metaphyseal region are strained differently.<sup>21</sup> While the calculation of strain in cancellous bone due to 0.3g oscillations is well beyond the scope of the present work, it is unlikely that the trabecular struts are subject to strains much beyond the 5  $\mu\epsilon$  to which the cortex endures, and certainly not in the yield region of the bone tissue. At this point, we can only presume that the interrelationship that persists between cortical and trabecular bone strain during the high-magnitude, low-frequency events is not disrupted in this lower strain magnitude domain.

It is also important to emphasize that this experiment was not designed to determine the degree to which transmissibility of the ground-based vertical oscillation diminishes as the signal travels proximally through the skeleton. Nevertheless, in a study measuring transmissibility in the hip and spine of human subjects

standing on the plate, it was shown that approximately 80% of a 30 Hz ground-based signal reached the hip and spine.<sup>32</sup> Therefore, although we anticipate that the strain signal may be larger toward the distal elements, a significant portion of that strain signal reaches the proximal femur.

Even if the strain within the trabeculae is not necessarily high, it is possible that other physical components of the mechanical environment are elevated due to the increase in frequency. Recent theoretical<sup>51</sup> work predicts, and empirical work<sup>33,34</sup> demonstrates, that byproducts of bone tissue deformation, such as fluid flow and intramedullary pressure, are strongly dependent on frequency. Keeping a strain signal constant (600  $\mu\epsilon$ ), but increasing the loading frequency from 0.1 to 10 Hz, elevates intramedullary pressure by an order of magnitude, and markedly increases fluid flow out of the bone. Thus, rather than deformation per se, these data support the notion that byproducts of the high-frequency strain signal, such as shear stress arising from fluid flow, or strain-generated potentials, may play an important role in regulating the adaptive response.

Cortical bone was not influenced by these low-level signals, a differential response also observed in shorter term rat<sup>45</sup> and mouse<sup>25</sup> studies. Whether this morphology-dependent response is because trabecular bone is metabolically more active, has a

**Table 4.** Comparative indices of static and dynamic histomorphometry of the proximal femur of experimental and control femora are shown following 1 year of mechanical stimulation

	Control	Experimental	Difference	P value
<b>Proximal femur</b>				
Bone volume/total volume (%)	15.2 ± 4.1	20.1 ± 4.8	+32%	0.04
Trabecular spacing ( $\mu\text{m}$ )	1170 ± 124	756 ± 97	-36%	0.02
Trabecular number	0.82 ± 0.16	1.19 ± 0.18	+45%	0.01
Trabecular thickness ( $\mu\text{m}$ )	191.3 ± 27.8	176.2 ± 14.9	-8%	0.22
Bone formation rate ( $\mu\text{m}^2/\text{mm}$ )	8.4 ± 12.7	17.9 ± 16.3	↑ 2.1-fold	0.19
Mineralizing surface (%)	2.6 ± 0.16	6.3 ± 5.14	↑ 2.4-fold	0.09
<b>Ultra distal radius</b>				
Bone volume/total volume (%)	28.9 ± 7.1	27.7 ± 3.5	-4%	NSD
Mineralizing surface (%)	2.5 ± 1.62	2.4 ± 1.28	-4%	NSD

These data substantiate the “whole bone” measurements made by pQCT, which demonstrated a 34% increase in bone density within the trabecular envelope. The 32% increase in bone volume was achieved both by a decrease in trabecular spacing and an increase in trabecular number. The diminished mean thickness of the trabeculae supports “new trabeculae” being formed. Together, the twofold increases in dynamic indices of bone formation, the longitudinal DXA data, the differences in static histomorphometry, and the strong osteogenic response observed in shorter term studies<sup>44</sup> all suggest that this low-level signal is anabolic. No significant differences (NSD) were measured in ulnae of either experimental or control animals.

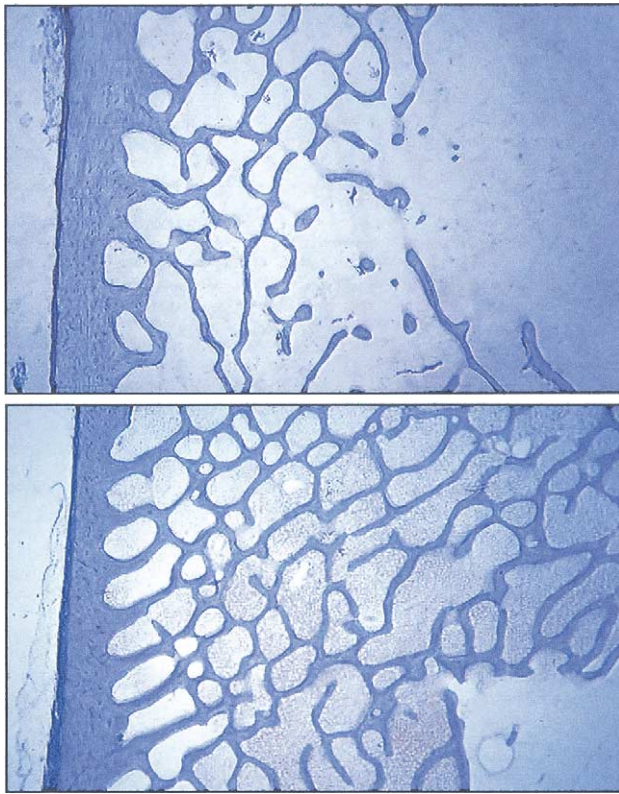


**Figure 2.** Photomicrographs of a region of the proximal sheep femur used for static histomorphometric evaluation of a control animal (top). One year of 20 min/day of a 0.3g, 30 Hz mechanical stimulus was anabolic to the bone (bottom), as shown by the higher number of trabecular elements.

greater cell density by virtue of a greater surface:volume ratio (i.e., more bone lining cells per unit volume), or that the endosteal compartment is exposed to distinct signals (e.g., intramedullary pressure), is unclear at this time. It is also important to note that the anabolic nature of the signal, resulting in a 32% increase in bone volume per total volume, conspiring toward a 27% improvement in trabecular bone strength in the longitudinal direction (of the distal femur<sup>43</sup>), was not readily detected by our DXA measurements. Thus, even though bone morphology and structure are being reinforced, bone density measurements were not sufficiently sensitive to identify these changes. Whereas at one level this implies that when DXA does identify change that the change is certainly relevant, it is also important to consider that both bone quantity and quality can change without detection by effective density measurements.

The data presented herein demonstrate that 20 min/day of these low-level signals is anabolic to bone, an observation supported by shorter term studies in rats,<sup>45</sup> which demonstrate that even 10 min/day can double both the bone formation rate and mineralizing surface after 4 weeks of exposure. With the rate of change of the DXA data significant in the tibia of the experimental group, and supported by the increase in bone volume per total volume and number of trabeculae in the femur, it can be seen that these mechanical stimuli effectively stimulate new bone formation in the skeleton subject to vertical oscillation. Although the increase in bone quantity could have been achieved solely via an anabolic response on the surfaces of existing trabeculae, that there is a decrease in spacing in parallel with a drop in trabecular width indicates the presence of new trabeculae,

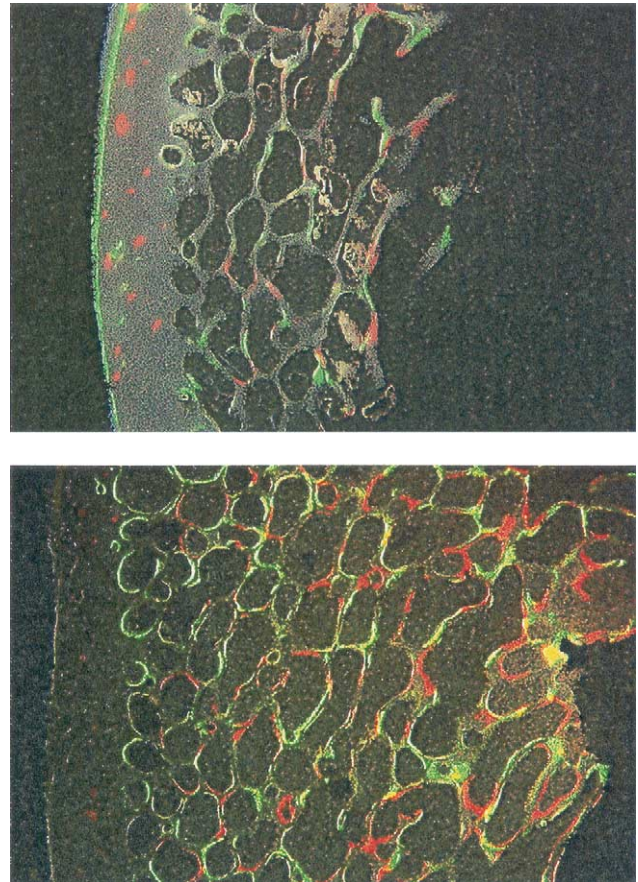


**Figure 3.** Fluorescent photomicrographs of anatomically similar regions of the proximal femur, comparing control (top) vs. experimental (bottom) animals. The 2.4-fold increase in mineralizing surface ( $p = 0.09$ ) was measured in animals subject to 20 min/day of a 0.3g, 30 Hz mechanical stimulus, indicating that more trabeculae from the experimental animals were actively involved in forming bone.

formed de novo as a result of the stimulus. The front limbs of the experimental animals, which were not subject to the mechanical stimulus, showed no change longitudinally (DXA) or as an endpoint (histomorphometry). These data suggest that mechanical factors work locally to regulate bone mass and morphology, and indicate that the adaptive process does not result in the release of a factor that systemically influences the skeleton.

If these low-level, high-frequency stimuli are critical determinants of bone mass and morphology, it becomes important to determine the origin of these dynamic strains and whether conditions of aging or menopause somehow alter these strain dynamics, and thus the etiology of the concomitant bone loss. Muscle mass is well known to decrease with age,<sup>49</sup> paralleled by a dramatic change in the dynamics of the muscle action.<sup>30</sup> A first order approximation of age-induced spectral changes in muscle dynamics was made by recording surface accelerations associated with postural muscle activity of the soleus,<sup>23</sup> a principal muscle associated with standing.<sup>12</sup> Spectra obtained from these recordings show that muscle activity in the frequency range  $>20$  Hz decreases by a factor of three in the elderly as compared with that seen in young adults, a response consistent with loss of fast oxidative-type fibers. As the high-frequency components seen in bone strain almost certainly arise through muscle activity, the deterioration of the postural muscle contraction spectra with age

would, therefore, contribute to a decrease in the strain spectral content at >20 Hz.

With the attenuation of spectral energy from muscle as a function of age, it can be argued that the sarcopenia that parallels aging also causes a significant loss of the mechanical signals that regulate bone, and thus muscle wasting is an etiologic factor in osteoporosis. Although the association between loss of muscle dynamics and bone mass is perhaps phenomenologic, it does indicate that the long-term demands that gravity places on postural muscle activity may represent a key factor in controlling bone mass.<sup>7</sup> This hypothesis is supported by measurements made from skeletal muscle harvested from rats flown in space. Exposure to weightlessness as for a time duration as brief as 7 days resulted in a 23% decrease in soleus muscle mass as compared with age- and weight-matched controls remaining on earth.<sup>14</sup> As the soleus is predominantly a postural muscle, and has a characteristic firing frequency of 20–25 Hz,<sup>20</sup> it could be argued that the absence of a need for posture reduces the demands made on the soleus, and thus extinguishes the key regulatory signal for the maintenance of bone mass, a signal that is not replaced even by intense exercise regimens entrained during spaceflight. Therefore, providing a vibration-based “surrogate” for the lost spectral strain history might inhibit osteoporosis. In support of this hypothesis, the rat-tail suspension model of disuse osteopenia was used to demonstrate that these low-level, high-frequency signals were capable of normalizing bone remodeling dynamics in animals subject to 23 h 50 min per day of disuse — an attribute that normal weight bearing for 10 min/day failed to accomplish.<sup>45</sup> In normal, fully ambulatory rats, the signal was strongly anabolic. However, this anabolic signal served only to normalize bone remodeling dynamics in animals subject to disuse, indicating the nature of regulatory signals in bone may shift if countering a strong catabolic stimulus.

Finally, it must be emphasized that the aim of the studies reported was to quantify the long-term adaptive response of cortical and trabecular bone to extremely low-level mechanical stimuli. These experiments were not designed to determine which cellular control mechanisms are, or are not, being utilized by the cells to effect these changes.<sup>4</sup> However, by demonstrating the strong anabolic potential of signals several orders of magnitude below those previously believed to be necessary to induce bone formation, some indication of the molecular means by which these cells perceive and respond to stimuli becomes possible.<sup>42</sup> Even in preliminary studies in the mouse, the differential response of cortical vs. trabecular bone is evident,<sup>25</sup> and the efficacy of the signal to modulate bone mass and morphology is mouse-strain-dependent, indicating not only physical influences on the adaptive response but also genomic factors. Functional genomic tools such as cDNA microarrays will ultimately help identify why one tissue type is more responsive than another,<sup>27</sup> and also why some skeletons are responsive to anabolic stimuli and others are not—thus, not only is bone strain important, but so is genomic strain.

In conclusion, these data demonstrate the anabolic potential of extremely low-level strain signals. That such low-level signals readily influence bone mass and morphology, it is reasonable to conclude that many aspects of vertebrate morphology may be as influenced by muscle architecture as by the intensity of load bearing. As importantly, the strong osteogenic capacity of these low-level signals suggests that a biomechanical intervention could provide a therapy for osteoporosis without the concomitant risks of pharmacologic treatment or exercise-induced injuries such as stress fractures or falls. The attributes of such biomechanical prophylaxes are that they are native to the bone tissue, they are safe at low intensities, the mechanical signals incorporate all aspects of a complex remodeling cycle,<sup>28</sup> will ultimately

induce lamellar bone,<sup>35</sup> and the relative amplitude of the signal will subside as formation persists.<sup>8</sup> Preliminary results from studies on postmenopausal women<sup>41</sup> and children with cerebral palsy<sup>50</sup> are encouraging in this regard.

---

*Acknowledgments:* The authors are grateful to the National Institutes of Arthritis, Musculoskeletal and Skin Diseases (AR-43498) for funding of this study, and to Exogen, Inc., for providing the oscillation devices. We are also grateful to J. Ryaby, T. Wilson, R. Talish, Y.-X. Qin, M. Strachan, T. Gladwell, and J. Rubin for their assistance with the protocol and their constructive comments on the manuscript, and to the numerous veterinary students at Colorado State University who spent countless hours monitoring the daily loading regimens.

---

## References

1. Adams, D., Spirt, A., Brown, T., Fritton, S., Rubin, C., and Brand, R. Testing the “daily stress stimulus” hypothesis of bone remodeling with natural and experimentally controlled strain histories. *J. Biomech* 30:671–678; 1997.
2. Bain, S., Impeduglia, T., and Rubin, C. Cement line staining in undecalcified thin sections of cortical bone. *Stain Technol* 65:1–5; 1990.
3. Bain, S. and Rubin, C. Metabolic modulation of disuse osteopenia: Endocrine dependent site specificity of bone remodeling. *J Bone Miner Res* 5:1069–1075; 1990.
4. Banes, A., Tsuzaki, M., Yamamoto, J., Fischer, T., Brown, T., and Miller, L. Mechanoreception at the cellular level. *Biochem Cell Biol* 73:349–365; 1995.
5. Biewener, A. Mechanics of mammalian terrestrial locomotion. *Science* 250: 1097–1103; 1990.
6. Blob, R. and Biewener, A. *In vivo* locomotor strain in the hindlimb bones of alligator mississippiensis and iguana iguana. *J Exp Biol* 202:1023–1046; 1999.
7. Booth, F. W. and Gollnick, P. D. Effects of disuse on the structure and function of skeletal muscle. *Med Sci Sports Exerc* 15:415–420; 1983.
8. Brown, T., Pedersen, D., Gray, M., Brand, R., and Rubin, C. T. Identification of mechanical parameters initiating periosteal remodeling. *J. Biomech* 23:893–905; 1990.
9. Burr, D., Martin, R., Schaffler, M., and Radin, E. Bone remodeling to in vivo fatigue microdamage. *J Biomech* 18:189–200; 1985.
10. Burr, D., Milgrom, C., Fyhrie, D., Forwood, M., Nyska, M., Finestone, A., Hoshaw, S., Saiag, E., and Simkin, A. In vivo measurement of human tibial strains during vigorous activity. *Bone* 18:405–410; 1996.
11. Carter, D., Harris, W., Vasu, R., and Caler, W. The mechanical and biological response of cortical bone to in vivo strain histories. In: Cowin, S., Ed. *Mechanical Properties of Bone*. New York: ASME; 1981; 81–95.
12. Clamann, H. Motor unit firing patterns in a human skeletal muscle. *Biophys J* 9:1233–1251; 1969.
13. Currey, J. *The Mechanical Adaptations of Bones*. Princeton, NJ: Princeton University; 1984.
14. Desplanches, D., Mayet, M. H., Ilyina-Kakueva, I., Sempore, B., and Flandrois, R. Skeletal muscle adaptation in rats flown on Cosmos 1667. *J Appl Physiol* 68:48–52; 1990.
15. Fritton, S., McLeod, K., and Rubin, C. Defining the 24-hour strain history of bone. *J Biomech* 33:317–326; 2000.
16. Fritton, S. and Rubin, C. T. In vivo Measurement of bone deformation using strain gages. In: Cowen, Ed. *Bone Mechanics*. Boca Raton, FL: CRC; 2001; 1–41.
17. Fritton, J., Rubin, C., Qin, Y., and McLeod, K. Vibration in the skeleton: I. Development of a resonance-based whole body vibration device. *Ann Biomed Eng* 25:831–839; 1997.
18. Frost, H. Skeletal structural adaptations to mechanical usage. *Anat Rec* 26: 403–413; 1990.
19. Fyhrie, D. and Carter, D. A unifying principle relating stress to trabecular bone morphology. *J Orthop Res* 4:304–317; 1986.
20. Hennig, R. and Lomo, T. Firing patterns of motor units in normal rats. *Nature* 314:164–166; 1985.
21. Hollister, S., Brennan, J., and Kikuchi, N. A homogenization sampling procedure for calculating trabecular bone effective stiffness and tissue level stress. *J Biomech* 27:433–444; 1994.
22. Hoshino, H., Kushida, K., Yamazaki, K. et al. Effect of physical activity as a caddie on ultrasound measurements of the os calcis: A cross-sectional comparison. *J Bone Miner Res* 11:412–418; 1996.

23. Huang, R., McLeod, K., and Rubin, C. Changes in the dynamics of muscle contraction as a function of age: A contributing factor to the etiology of osteoporosis? *J Gerontol* 54:352–357; 1999.
24. Hylander, W., Ravosa, M., Ross, C., and Johnson, K. Mandibular corpus strain in primates: Further evidence for a functional link between symphyseal fusion and jaw-adductor muscle force. *Am J Phys Anthropol* 107:257–271; 1998.
25. Judex, S., Xu, G., Donahue, L. R., Hadjiargyrou, M., and Rubin C. T. Changes in trabecular bone formation induced by mechanical stimulation and disuse are accompanied by differential gene expression in a mouse. *Trans Orthop Res Soc* 47:533; 2001.
26. Littell, R. C., Milliken, G. A., Stroup, W. W., and Wolfinger, R. D. *The SAS System for Mixed Models*. Cary, NC: SAS; 1996.
27. Lombardo, F., White, D., Dhundale, A., Rubin, C. T., and Hadjiargyrou, M. Transcriptional profiling of the early phases of bone regeneration via cDNA library construction and custom microarrays. *Trans Am Soc Bone Miner Res*. In press.
28. Martin, R., Burr, D., and Sharkey, N. *Skeletal Tissue Mechanics*. New York: Springer; 1998.
29. McLeod, K. and Rubin, C. Efficacy of very low frequency electric fields in the regulation of bone remodeling activity. *J Bone Jt Surg* 74:920–929; 1992.
30. Orizio, C. Muscle sound: Bases for mechanomyographic analyses. *Crit Rev Biomed Eng* 21:201–243, 1993.
31. Parfitt, A., Drezner, M., Glorieux, F., Kanis, J., Malluche, H., Meunier, P., Ott, S., and Recker, R. R. Bone histomorphometry: Standardization of nomenclature and units. *J Bone Miner Res* 2:595–610; 1987.
32. Pope, M. H., McLeod, K., Magnusson, M., Rostedt, M., Hansson, T., and Rubin, C. Transmission of whole body vibrations in the 10–40 Hz range into the hip and lumbar spine. *Trans Orthop Res Soc* 21:668; 1996.
33. Qin, Y.-X., Rubin, C., and McLeod, K. Nonlinear dependence of loading intensity and cycle number in the maintenance of bone mass and morphology. *J Orthop Res* 16:482–489; 1998.
34. Qin, Y.-X., Lin, W., and Rubin, C. The relationship between bone fluid flow and adaptation as stimulated by intramedullary hydraulic loading. *Trans Orth Res Soc* 26:319; 2001.
35. Rubin, C., Gross, T., McLeod, K., and Bain, S. Morphologic stages in lamellar bone formation stimulated by a potent mechanical stimulus. *J Bone Miner Res* 10:488–495; 1995.
36. Rubin, C. and Lanyon, L. Limb mechanics as a function of speed and gait: A study of functional strains in the radius and tibia of horse and dog. *J Exp Biol* 101:187–221; 1982.
37. Rubin, C. and Lanyon, L. Regulation of bone formation by applied dynamic loads. *J Bone Jt Surg* 66:397–402; 1984.
38. Rubin, C. and Lanyon, L. Dynamic strain similarity in vertebrates: An alternative to allometric limb bone scaling. *J Theor Biol* 107:321–327; 1984.
39. Rubin, C. and Lanyon, L. Regulation of bone mass by mechanical strain magnitude. *Calcif Tissue Int* 37:411–417; 1985.
40. Rubin, C. and McLeod, K. Promotion of bony ingrowth by frequency specific, low amplitude mechanical strains. *Clin Orthop Rel Res* 298:165–174; 1994.
41. Rubin, C., Recker, R., Cullen, D., Ryaby, J., and McLeod, K. Prevention of bone loss in a post-menopausal population by low-level biomechanical intervention. *Am Soc Bone Miner Res* 23:1106; 1998.
42. Rubin, C., Sun, Y.-Q., Hadjiargyrou, M., and McLeod, K. Increased expression of matrix metalloproteinase-1 mRNA in osteocytes precedes bone resorption as stimulated by disuse: Evidence for autoregulation of the cell's mechanical environment? *J Orthop Res* 17:354–361; 1999.
43. Rubin, C., Turner, A.S., Müller, R., Mitra, E., Lin, W., McLeod, K., and Qin, Y.-X. Quantity and quality of trabecular bone in the femur are enhanced by a strongly anabolic, non-invasive mechanical intervention. *J Bone Miner Res*. In press.
44. Rubin, C., Turner, A. S., Bain, S., Mallinckrodt, C., and McLeod, K. Anabolism: Low mechanical signals strengthen long bones. *Nature* 412:603–604; 2001.
45. Rubin, C., Xu, G., and Judex, S. The anabolic activity of bone tissue, suppressed by disuse, is normalized by brief exposure to extremely low magnitude mechanical stimuli. *FASEB J* 15: 2225–2229; 2001.
46. Schaffler, M., Radin, E., and Burr, D. Long-term fatigue behavior of compact bone at low strain magnitude and rate. *Bone* 11:321–326; 1990.
47. Snow-Harter, C., Bouxsein, M., Lewis, B., Carter, D., and Marcus, R. Effects of resistance and endurance exercise on bone mineral status of young women. *J Bone Miner Res* 7:761–769; 1992.
48. Turner, A. S., Mallinckrodt, C. H., Alvis, M. R., and Bryant, H. U. Dual-energy x-ray absorptiometry in sheep: Experiences with in vivo and ex vivo studies. *Bone* 17:381–387; 1995.
49. Tzankoff, S. and Norris, A. Effect of muscle mass decrease on age-related BMR changes. *J Appl Phys* 43:1001–1006; 1977.
50. Ward, K., Alsop, C., Brown, S., Caulton, J., Adams, J., and Mughal, M. A randomized, placebo controlled, pilot trial of low magnitude, high frequency loading treatment of children with disabling conditions who also have low bone mineral density. *Trans Am Soc Bone Miner Res* 16(Suppl.):1148; 2001.
51. Weinbaum, W., Cowin, S., and Zeng, Y. A model for the excitation of osteocytes by mechanical loading-induced bone fluid shear stresses. *J Biomech* 27:339–360; 1994.
52. Wolff, J. *The Law of Bone Remodeling*. Translated by Maquet, P. and Furlong, R. Berlin: Springer; 1986.

---

*Date Received* : June 22, 2001

*Date Revised*: October 12, 2001

*Date Accepted*: October 19, 2001